Photochemistry and Photobiology, 20**, **: *–*

Research Article

6-Nitro-Quinazolin−4(3*H*)−one Exhibits Photodynamic Effects and Photodegrades Human Melanoma Cell Lines. A Study on the Photoreactivity of Simple Quinazolin−4(3*H*)−ones

Anastasios Panagopoulos[1†], Thomas Balalas[2†], Achilleas Mitrakas[3], Vassilios Vrazas[4], Katerina R. Katsani[4], Alexandros E. Koumbis[2], Michael I. Koukourakis[3], Konstantinos E. Litinas[2] and Konstantina C. Fylaktakidou[1,2]*

[1]Laboratory of Organic, Bioorganic and Natural Product Chemistry, Molecular Biology and Genetics Department, Democritus University of Thrace, Dragana, Alexandroupolis, Greece
[2]Laboratory of Organic Chemistry, Chemistry Department, Aristotle University of Thessaloniki, Thessaloniki, Greece
[3]Department of Radiotherapy/Oncology, Democritus University of Thrace/University General Hospital of Alexandroupolis, Alexandroupolis, Greece
[4]Laboratory of Biochemistry and Molecular Virology, Molecular Biology and Genetics Department, Democritus University of Thrace, Dragana, Alexandroupolis, Greece

Received 16 October 2020, accepted 29 December 2020, DOI: 10.1111/php.13376

ABSTRACT

Photochemo and photodynamic therapies are minimally invasive approaches for the treatment of cancers and powerful weapons for competing bacterial resistance to antibiotics. Synthetic and naturally occurring quinazolinones are considered privileged anticancer and antibacterial agents, with several of them to have emerged as commercially available drugs. In the present study, applying a single-step green microwave irradiation mediated protocol we have synthesized eleven quinazolinon−4(3*H*)−ones, from cheap readily available anthranilic acids, in very good yields and purity. These products were irradiated in the presence of pBR322 plasmid DNA under UVB, UVA and visible light. Four of the compounds proved to be very effective DNA photocleavers, at low concentrations, being time and concentration dependent as well as pH independent. Participation of reactive oxygen species was related to the substitution of quinazolinone derivatives. 6-Nitro-quinazolinone in combination with UVA irradiation was found to be *in vitro* photodestructive for three cell lines; glioblastoma (U87MG and T98G) and mainly melanoma (A−375). Thus, certain appropriately substituted quinazolinones may serve as new lead photosensitizers for the development of promising biotechnological applications and as novel photochemo and photodynamic therapeutics.

INTRODUCTION

Photochemo therapy (1,2) and photodynamic therapy (3–8) are considered minimally invasive approaches for alternative or adjuvant to classical chemotherapeutic, radiotherapeutic or surgical therapies of several kinds of cancers and other nonmalignant diseases. They usually depend on the excitation of a chemical compound, a "photosensitizer," which absorbs light of a specific wavelength and triggers a series of cascade reactions able to destroy "on-demand" biological targets, both in a spatial and a temporal way.

Moreover, biotechnological phototriggered studies are currently exploding focusing on approaches which aim to give solutions in critical problems, for example inhibition of teratoma in stem cell regeneration therapy (9) or improvement of drug delivery via visible light-triggered intracellular co-delivery and photocleavage of linkers (10). Finally, photosensitizing techniques are used in the fields of bioimaging and photocatalysis (11,12).

As far as therapeutic approaches are concerned, the efficiency of the treatments depends not only on the properties of the photosensitizer but also on the characteristics of the irradiated area and the wavelength of light irradiation. UVB (290−315 nm) and UVA (315−400 nm), or a combination of them, find extensive applications mainly, but not exclusively, in dermatology (13–15). Some characteristic examples are referred to the treatment of psoriasis (16,17) and vitiligo (18,19), palmoplantar pustulosis (20), early-stage mycosis fungoides (21), T-cell-mediated diseases (22), pityriasis (23), etc. The visible area of the light spectrum is currently used for the photodynamic therapy of multiple actinic keratoses (24,25), Bowen's disease and basal cell carcinoma (26,27), melanotic melanoma (28), acne vulgaris (29), to mention few.

Photosensitizers are also used for the photoinactivation of bacteria (PIB). This approach seems to be highly promising, as one of the last lines of defense for the fight against bacteria resistance to antibiotics. Development of PIB procedures shows, at the moment, no obvious risk to reach new dead ends (30–32), due to the fact that the reactive radical species created by the photosensitizers attack multiple biological targets on bacteria.

Several organic compounds, bearing quite diverse structures, have been identified as DNA photocleavaging agents. These

*Corresponding author email: kfylakta@chem.auth.gr (Konstantina C. Fylaktakidou)
†The authors contributed equally to this work.

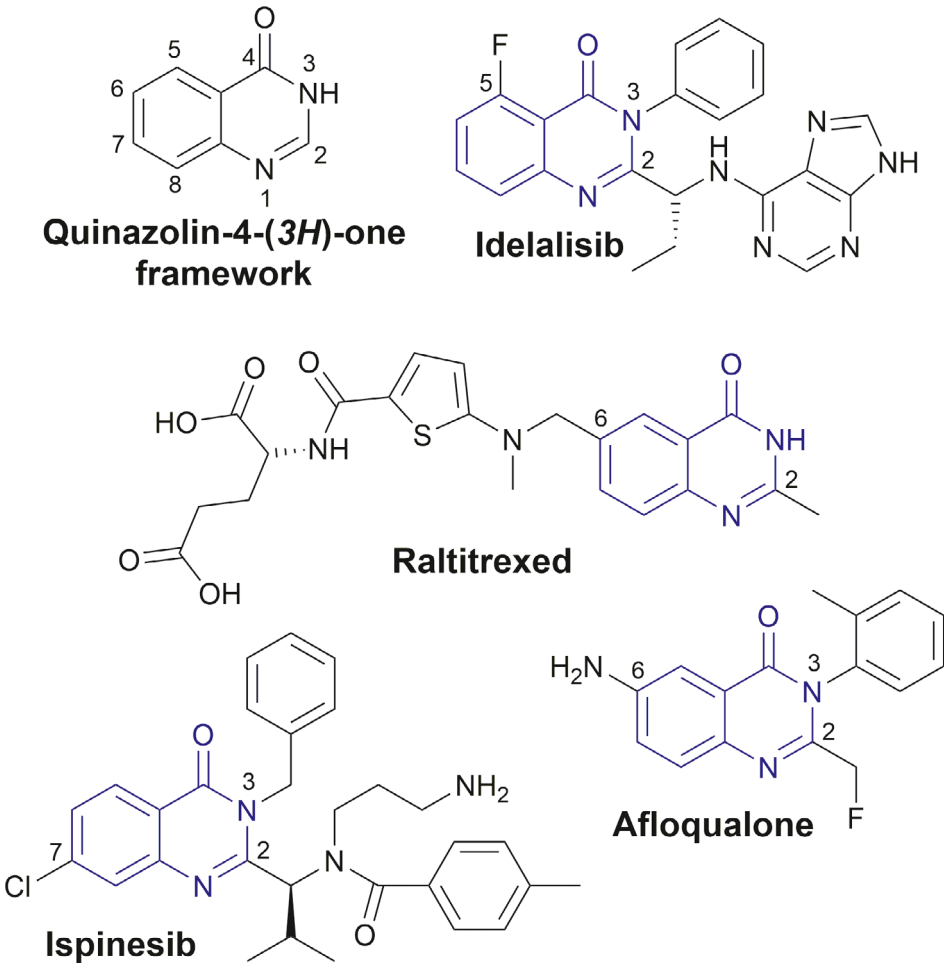

Figure 1. Structures of parent quinazolin−4−(3*H*)−one and commercially available drugs containing quinozalinone scaffold.

include [1,2,4]−triazolo−[4,3−a]quinoxalines (33), quinoxalin−4(5*H*)−ones (34), enediynes (35,36), pyrrolecarboxamide conjugated 4′−bromo−acetophenones (37), halophenyl sulfonamide derivatives of poly *N*−methylimidazoles (38), naphthalimides, (39–41) nitrobenzamido amino-acridine derivatives (42,43), benzo[*b*][1,8]naphthyridines (44) and quinolones (45–47), *N*−phenylhydroxylamine derivatives (48), *O*−acyl (49–53), *O*−sulphonyl (54,55) and *O*-carbamoyl (56) oximes, β−carbolines (57,58), pyrazole derivatives (59,60), azido carbonyl compounds (61), etc.

Quinazolinones represent ubiquitous structural scaffolds in medicinal chemistry which are profoundly considered as "privileged structures." Not surprisingly, they serve as building blocks for approximately 150 naturally occurring alkaloids isolated from a number of families of the plant kingdom, from microorganisms and animals. Additionally, at least 10 commercially available drugs used in clinical therapy, such as afloqualone, ispinesib, raltitrexed and idelalisib (Fig. 1), feature as pharmacophore the quinazolinone moiety. As a result, both synthetic approaches and the observed biological activities (anti-inflammatory, anti-cancer, anti-microbial, anti-convulsant, anti-hypertensive, anti-diabetic etc) for quinozalinones have been extensively reviewed (62–67). Within those studies, some derivatives proved to be DNA binding and cleaving agents (68–70).

Photostability of drugs is considered important in order to avoid side effects; nevertheless photosensitivity is the demanded activity for phototherapeutic applications and protocols. In the literature, photochemical experiments on quinazolinones afforded *syn-anti* photoisomerizations of arylethylene derivatives (71,72) or Schiff bases (73). A recent photophysical study on some quinazolinone scaffolds has shown a high photostability (74). As far as photobiological experiment concerns, a certain derivative and more specifically, the central nervous acting muscle relaxant drug "Afloqualone (AFQ)," (75) Fig. 1, caused photosensitive skin reactions upon administration. The drug was phototoxic to bacteriophage lambda (76), and it was exhibiting DNA photocleavage activity by photodynamic action (77,78). Our team has incorporated metal complexation in properly designed quinazolinone scaffolds and identified photosensitivity owed to the metal excitation (79,80). It seems to us that photosensitization of this important class of compounds represents an active field, not only in terms of the behavior of quinazolinones toward metal complexation, but also in terms of the photoeffects of the substituents on this pharmacophore scaffold, which are, to the best of our knowledge, rarely explored. Thus, due to our continuous interest in the discovery of organic molecules acting as photosensitizers and DNA photocleavers (53–56) we have initiated a quinazolinone-related project, and investigated photosensitization,

photodisrupting and photodynamic effects of various substituents on this pharmaceutical frame. In our designing, halogens and nitro groups, as well as hydroxyl and methyl groups at different positions of the aromatic framework were incorporated.

All compounds were synthesized using a green microwave-assisted protocol, isolated in very high yields and screened under UVB irradiation in the presence of supercoiled plasmid DNA pBR322 in order to investigate their efficacy to photoreact. UV absorption at higher wavelengths was the factor that allowed the study with UVA and visible light. For the compounds that showed the highest DNA photocleavage activity, the photochemistry and mechanism of action in the presence of DNA using various scavengers were studied. Finally, glioblastoma cell lines U87MG and T98G (ATCC® HTB−14™ and ATCC® CRL−1690™, respectively) and skin malignant melanoma cell line A−375 (ATCC® CRL−1619™) were treated with the compound that presented overall the best activity, *in vitro*.

MATERIALS AND METHODS

All commercially available reagent-grade chemicals and solvents were used without further purification. pB322 supercoiled plasmid was purchased from New England Biolabs. NMR spectra were recorded on an Agilent 500/54 (500 MHz, 125 MHz and 470 MHz for ^{1}H, ^{13}C and ^{19}F, respectively) spectrometer using $CDCl_3$, and/or DMSO − d6 as solvent. *J* values are reported in Hz. Mass spectra were determined using a Shimadzu LCMS−2010 EV system under electrospray ionization (see Supporting Information) conditions. All samples containing pBR322 plasmid were irradiated at pH 6.8 with Philips 2 × 9W/01/2P UV−B narrowband lamps at 312 nm, Philips 2 × 9W/10/2P UV−A lamps at 365 nm or white light OSRAM DULUX S BLUE. The same lamps were used for the irradiation in solutions without the plasmid. UV–vis spectra were recorded on a Hitachi U–2001 dual-beam spectrophotometer. Fluorescence spectra were recorded in solution on a Hitachi F-7000 fluorescence spectrophotometer. MW experiments were performed on a scientific focused microwave reactor (Biotage Initiator 2.0). All reactions were monitored on commercially available precoated TLC plates (layer thickness 0.25 mm) of Kieselgel 60 F_{254}. Calculation of yields was based on the amount of the directly crystallized product.

General procedure for the synthesis of quinazolinones 12−22. The commercially available anthranilic acids **1**−**11** (1 mmol) were individually mixed with triethyl orthoformate (1.3 mmol) and ammonium acetate (1.3 mmol) in the presence of 95% EtOH (0.5 mL). The mixture was irradiated for 20 min at 110 °C and then allowed to cool to room temperature. 95% EtOH (0.5 mL) was added and the resulting suspension was filtered under reduced pressure. The obtained product was dried under vacuum and was used without any further purification. (See Supporting Information for references, data analysis and crude spectra).

DNA photocleavage experiments. Cleavage of supercoiled circular pB322 DNA by Quinazolinones 12−22. Compounds **12**−**22** were individually incubated with plasmid DNA at the desired concentration, in pyrex vials (10 mm diameter) and were irradiated with UV−Visible light (312 nm−18 W, or 365 nm−18 W, or visible light 400−700nm−18W) under aerobic conditions at room temperature for 30 min and in 15 cm distance (312 nm), or 2 h and in 10 cm distance (365 nm), or 2 h and in 10 cm distance (visible light). Conditions of the photobiological reaction and gel electrophoresis, quantification of DNA-cleaving activity and calculation of ss% and ds% damage protocols have been described previously (53). All experiments were performed at least three times.

Photochemical experiments. UV irradiations in DMSO−d_6. Pyrex vials containing samples of **15** and **18** were individually dissolved in DMSO−d_6 and the solutions were irradiated at 312 nm for 30, 60 and 120 min under air. Additionally, another series of same solutions were extensively degassed with argon, for at least one hour and then irradiated for the same time intervals as the solutions before. Finally, ^{1}H−NMR spectroscopy was used to analyze all samples and the changes were comparatively studied.

UV irradiations in Benzene. Pyrex vials containing samples of **15**, **18** and **20** (5 mg) were individually dissolved in dry benzene (2 mL) and the mixture was degassed with argon for at least 1 h. 1,4−cyclohexadiene (50 μL) was added and the mixture was irradiated for 2 h at 312 nm (2 × 9 W, 5 cm distance). After completion of the experiment, the solvent was removed under vacuum and a reaction sample was analyzed by ^{1}H−NMR and LC−MS (52,54).

UV irradiations in MeOH/H_2O. Pyrex vials containing samples of **15**, **18** and **20** (5 mg) were individually dissolved in MeOH/H_2O (9/1) (3 mL). The mixture was degassed with argon for at least 1 h and then irradiated for 2 h at 312 nm or 365 nm (2 × 9 W, 5 cm distance). After completion of the experiment, the solvent was removed under vacuum and a reaction sample was analyzed by ^{1}H−NMR and LC−MS. (52,54)

Biological assays. Cell culture experiments. Glioblastoma cell lines U87MG and T98G (ATCC® HTB−14™ and ATCC® CRL−1690™, respectively) and skin malignant melanoma cell line A−375 (ATCC® CRL−1619™) were used for these experiments. Cells were cultured under aseptic conditions using DMEM basal medium (31885-023; Gibco) supplemented with 10% fetal bovine serum (FB−1000/500, Biosera, UK), 100 units/ml Penicillin and 100 μg mL^{-1} Streptomycin (15140−122, Gibco) and 2mM L−Glutamine (25030; Gibco). Both cell lines were maintained at standard conditions (37°C, 5% CO_2) in humidified atmosphere and were used upon reaching 70–90% confluency. The proper concentration of **15** was found using titrations with seven concentrations (0−1 mM). Fluorescence measurements have been performed using Resazurin Cell Viability Assay (CA035, Canvax, Spain) as next described. For the measurement of the cytotoxic effect of compound **15**, 500 cells/well for T98G and U87MG cell lines and 2000 cells/well for A-375 cell line were seeded in a 96-well plate. Cells were incubated for 30 min with 50 μM of **15** and fresh medium was added before irradiation. Then, cells were irradiated using a radiation source which emitted a wavelength of 365 nm (UVA). UVA lamp was placed 10 cm over the 96-well plate. Resazurin was added 24 h after irradiation. A nonirradiated 96-well plate was used as a control, under the same conditions (81,82).

Resazurin cell viability assay. Incubation with 10% resazurin (7 h) was followed by fluorescence measurement using 590 nm as emission wavelength and 530−560 nm as excitation wavelength in a FLUOstar Omega microplate reader (BMG LABTECH GmbH, Ortenberg, Germany). Moreover, culture medium was used as negative control while 5% vitamin C was used as positive control for the full reduction of resazurin.

RESULTS AND DISCUSSION

Synthetic procedure

Commercially available anthranilic acids **1**−**11**, triethyl orthoformate and ammonium acetate were added in EtOH. The reaction mixture for each starting anthranilic acid was subjected to microwave irradiation for 20 min at 110°C, resulting in very good yields a single product (**12**−**22**, Scheme 1), which was completely dissolved in the hot reaction mixture. Upon cooling to room temperature, simple filtration of the precipitated solid and washing with cold EtOH gave the desired products which needed no further purification since the byproducts of the reactions (EtOH and AcOH) were completely removed.

The microwave-assisted reaction of anthranilic acid **1**, triethyl orthoformate and ammonium acetate for the synthesis of **12** was previously performed, solvent-free, in a domestic microwave oven giving the product in excellent yield and purity (83). The focus of that approach was on the preparation of five alkyl or phenyl quinazolinone derivatives altered on position 2 of the scaffold. Within this manuscript, the scope of the reaction has been extended, using a variety of additional 10 anthranilic acids, substituted on the aromatic ring with electron donating or withdrawing groups, using a scientific microwave reactor.

The use of a minimum amount of ethanol as solvent, demonstrates the green dimension of this approach, since the same

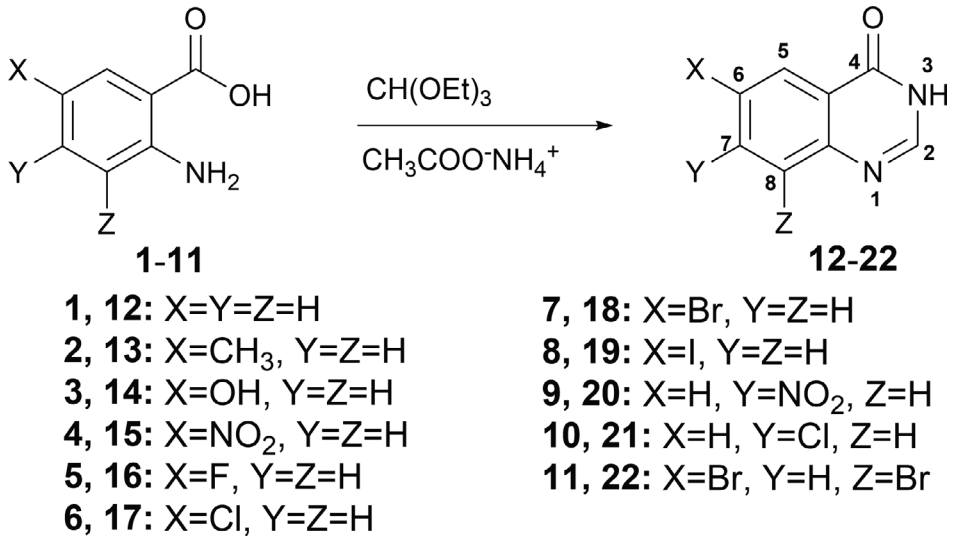

Scheme 1. Synthesis of quinazolin−4−(3*H*)−ones **12**−**22**. Reagents and conditions: anthranilic acid **1**−**11**, triethyl orthoformate, ammonium acetate, 20 min, 110°C, EtOH.

solvent is simultaneously used for the crystallization of the quinazolinone products, providing pure crystals of compounds **12**–**22** upon cooling of the reaction mixture. Their ^{1}H and ^{13}C−NMR spectra (see Supporting Information) are in full accordance with those reported in the literature. (84,85) By performing this green and efficient synthesis of the simplest quinazolinones with diverse substitution pattern on the aromatic ring, we set up the basis for their photochemical and photobiological study.

DNA photocleavage experiments

One of the most feasible experiments for the discovery of photosensitizers with biological interest seems to be the identification of DNA "photocleavers," (86,87) which *via* various mechanistic pathways may lead to single-stranded (ss) DNA damage, repairable by enzymatic processes and/or double-stranded (ds) DNA photocleavage (88,89). The requirement for the activity of the photosensitizer is, besides the ability to be excited at a specific light wavelength, the affinity to DNA (53,86), which maybe expressed *via* intermolecular forces or intercalation. The fact that these forces could be applicable to other biological targets renders DNA photocleavage identification a multi-informative procedure, useful both in chemistry and in biology.

The designing of the experiments included the preliminary screening of compounds **12**–**22** in DMSO solutions (500 μμ) up to 10% in a Tris buffer solution (25 μM, pH = 6.8) containing the supercoiled circular pBR322 DNA (Form I). Their screening involved UVB (312 nm) or UVA (365 nm) irradiation for 30 min and 2 h, respectively, at room temperature under aerobic conditions. Compounds **15**, **18** and **19** showed considerable activity, whereas quinazolinones **17** and **22** showed low to moderate activity at this concentration at 312 nm (Fig. 2, Lanes 6, 9, 10, 8 and 13, respectively).

As it is observed in Fig. 2, 6−nitro−quinazolinone **15** degraded completely plasmid DNA, designating this compound as a very efficient one. On the contrary, 7−nitro−quinazolinone **20** showed no activity (Lanes 6 and 11, respectively). Nevertheless, the latter compound cleaved DNA at higher concentration (1 mM) giving the nicked form (100%), probably due to its lower UV absorption in this irradiation area. The rest of the inactive compounds showed no improvement under the same conditions (data not shown). It is worth mentioning that the position of nitro group in photosensitizers seems to be crucial for the outcome of the photocleavage, as it was reported for various derivatives. However, due to the diversity of those substrates (naphthalimides, nitrobenzamidoacridines and *N*-methyl-pyrrolecarboxamides) a prediction of the role of the position may lead

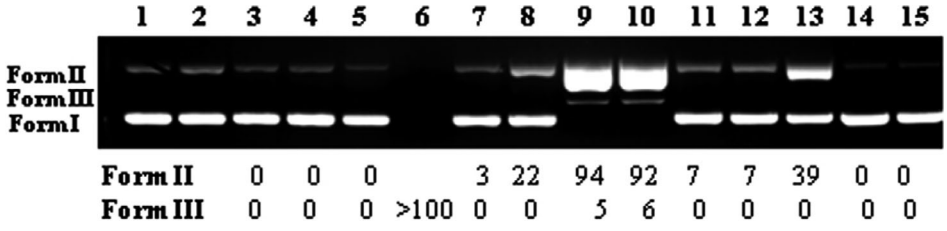

Figure 2. Efficiency of quinazolinones **12**−**22** on DNA photocleavage. Gel electrophoresis image (GEI): Lanes 1 and 2: Control plasmid pBR322 and control pBR322 irradiated; Lanes 3–13: pBR322 + one of quinazolinones (**12** or **13**, or **14**, or **15**, or **16**, or **17**, or **18**, or **19**, or **20**, or **21**, or **22**, respectively) + UV irradiation; Lanes 14 and 15: pBR322 + DMSO (10% and 20%, respectively) + UV irradiation. Calculation % of the formation of nicked (Form II) and linear (Form III) pBR322 is given at the bottom of the image (53).

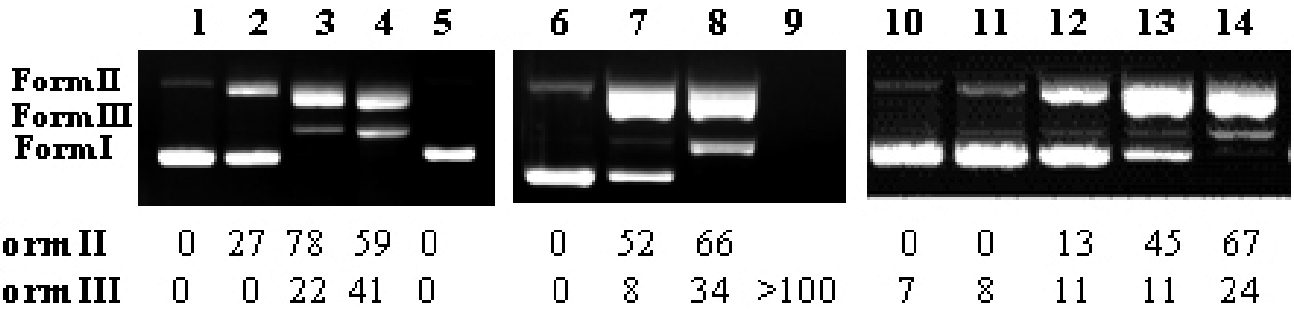

Figure 3. Concentration dependence DNA photocleavage of quinazolinones **15** and **20**. GEI: **Left:** 312 nm; Lanes 1–4: pBR322 + **15** (1 or 10, or 50, or 100 μμ, respectively) + UV irradiation; Lane 5: pBR322 + **15** (500 μμ) DARK; **Center:** 365 nm; Lanes 6–9: pBR322 + **15** (1 or 10, or 25, or 50 μμ, respectively) + UV irradiation; **Right:** 365 nm; Lanes 10–14: pBR322 + **20** (1 or 10, or 25, or 50, or 100 μM, respectively) + UV irradiation. For calculations see comment in Fig. 2.

to uncertain conclusions and, thus, for the moment this seems to be a case study for each class of compounds. (41,42,60) As far as the halogenated compounds concerns, we observed that 6−fluoro quinazolinone **16** has a negligible activity, which was slightly improved when fluorine was replaced by chlorine (**17**) and this trend reached the top of activity almost equally for 6−bromo (**18**) and 6−iodo−quinozalinone (**19**), Fig. 2 (Lanes 7, 8, 9 and 10, respectively).

It is interesting to note that the activity was almost lost when chlorine was found at position 7 of the quinazolinone aromatic ring instead of position 6 (Lanes 8 and 12, respectively), similarly to the results observed for compounds **15** and **20**. Additionally, the introduction of a second atom of bromine led to the loss of almost half of the activity as compared to the activity of compound **18** (Lanes 13 and 9, respectively).

Irradiation at 365 nm was applied to compounds **13**, **15**, **16** and **20** since they absorb UV light even slightly at this wavelength (Supporting Information, Figure S3), with derivatives **15** and **20** to absorb notably high, due to their chromophore, the nitro group. The latter compounds degraded the pBR322 plasmid at 500 μM to such an extent that ethidium bromide did not detect any plasmid fragment. Thus, the effective concentration for photocleavage of the 50% of DNA was tested for derivative **15** at 312 and 365 nm and for **20** at 365 nm, Fig. 3.

For derivative **15** this concentration was between 10 and 50 μμ at 312 nm (Fig. 3, Lanes 2 and 3) and at *ca*. 10 μμ at 365 nm (Lane 7). Compound **20** destroyed 50% of the plasmid DNA at *ca*. 50 μμ (Lane 13). Quinazolinone **15** was found to be inactive in dark, without UV irradiation (Lane 5). Additionally, none of the tested compounds showed any activity toward DNA in the absence of UV irradiation. The effective concentration for photocleavage of the 50% of DNA caused by compound **18** was 100 μμ (data not shown), which is rather high and may be attributed to the different mechanism of action, compared to compound **15** at 312 nm (*vide infra*).

Compounds showing the optimum DNA photocleavage at UVA irradiation and absorption behind 365 nm were also examined under visible light (Fig. 4). 6-Nitro-quinazolinone (**15**) exhibited activity at 250 μμ (Lane 2). This was gradually and linearly progressed degrading completely DNA at 500 μM and behind. There was no activity in dark at 1000 μμ (Lane 6). On the contrary, although compound **20** was relatively active at 365 nm, the same linearity between concentration and activity was not observed (Fig. 4, Lanes 8-10), probably due to its generally lower photoreactivity compared to that of **15**.

We next examined the mechanism of action and the dependence on pH of the most active compounds **15**, **18** and **20** under irradiation at various wavelengths. The activity of **15** against DNA did not show any change in a wide range of pH (50 μμ concentration, pH 5 to 10, see Supporting Information, Figure S4.1). Concerning the mechanism of action, it seems that oxygen plays an important role for the nitro derivatives, whereas Br compound **18** showed certain differences. As it is observed in Figs. 5 and 6, compound **15** follows the same mode of action under all tested irradiation wavelengths (312 nm, 365 nm and visible light). Under argon, the DNA photocleavage was notably decreased [Fig. 5, Lanes 3 (312 nm) and 11 (365 nm), and Fig. 6, Lane 2 (visible light)]. The implication of radicals is obvious, since the activity was again diminished in the presence of scavengers, such as *L*−cysteine and potassium iodide. We observed no activity of **15** in the presence of the singlet oxygen scavenger NaN_3, an indication that singlet oxygen is involved, although there was no change in the presence of D_2O [NaN_3: Fig. 5, Lanes 6 (312 nm) and 14 (365 nm), and Fig. 6, Lane 5

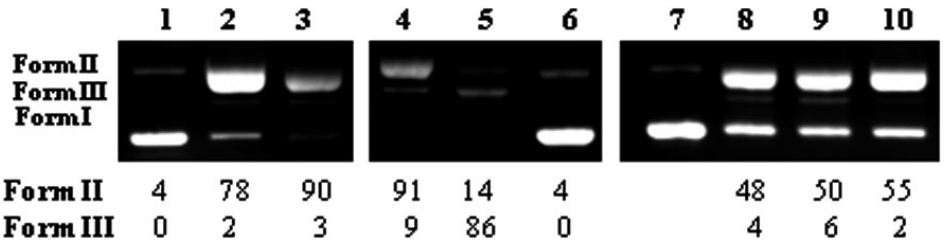

Figure 4. Concentration dependence DNA photocleavage of quinazolinones **15** and **20** under visible light. GEI: **Left and Center:** Lanes 1–5: pBR322 + **15** (50 or 250, or 500, or 600, or 800 μμ, respectively) + UV irradiation; Lane 6: pBR322 + **15** (1000 μμ) DARK; **Right:** Lane 7: Control plasmid pBR322 irradiated; Lanes 8–10: pBR322 + **20** (1000 or 750, or 500 μμ, respectively) + UV irradiation. For calculations, see comment in Fig. 2.

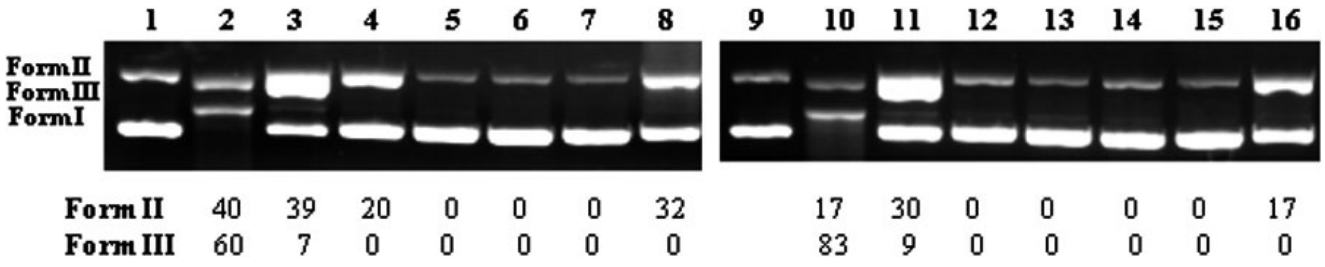

Figure 5. Mechanistic studies for quinazolinone **15**. GEI: **Left image:** 312 nm (50 μM). **Right image:** 365 nm (25 μμ). Lanes 1 and 9 are control plasmid DNA + UV irradiation; Lanes 2 and 10: pBR322 + **15** + UV; Lanes 3 and 11: pBR322 + **15** + UV + Argon; Lanes 4 and 12: pBR322 + **15** + UV + *L*−cysteine (1500 μμ); Lanes 5 and 13: pBR322 + **15** + UV + KI (250 μμ); Lanes 6 and 14: pBR322 + **15** + UV + NaN_3 (20 mμ); Lanes 7 and 15: pBR322 + **15** + UV + D_2O; Lanes 8 and 16: pBR322 + **15** + UV + DMSO (20 μμ). For calculations see comment in Fig. 2.

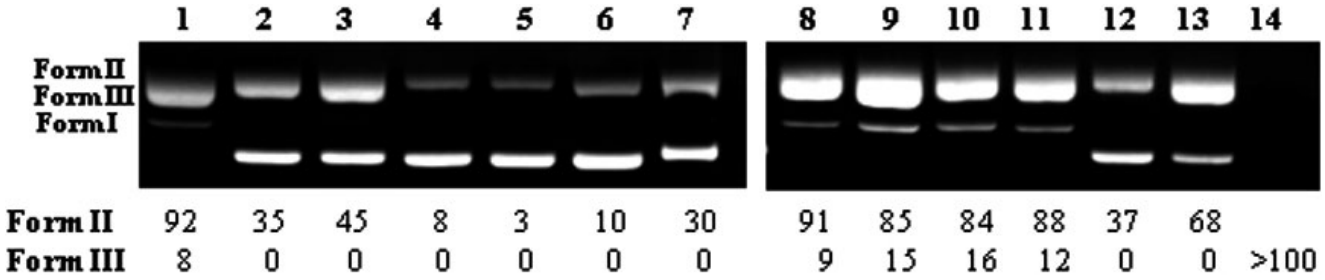

Figure 6. Mechanistic studies for quinazolinones **15** and **18**. GEI: **Left image:** Visible light (400−750 nm), (**15**, 600 μμ). **Right image:** 312 nm (**18**, 500 μμ). Lanes 1 and 8: pBR322 + **15** or **18** + light; Lanes 2 and 9: pBR322 + **15** or **18** + light + argon; Lanes 3 and 10: pBR322 + **15** or **18** + light + *L*−cysteine (1500 μM); Lanes 4 and 11: pBR322 + **15** or **18** + light + KI (250 μμ); Lanes 5 and 12: pBR322 + **15** or **18** + light + NaN_3 (20 mμ); Lanes 6 and 13: pBR322 + **15** or **18** + light + D_2O; Lanes 7 and 14: pBR322 + **15** or **18** + light + DMSO (20 μμ). For calculations see comment in Fig. 2.

(visible light); D_2O: Fig. 5, Lanes 7 (312 nm) and 15 (365 nm), and Fig. 6, Lane 6 (visible light)]. The presence of hydroxyl radicals, $^{\cdot}OH$, is also evidenced by the reduction of the activity in the presence of 20% DMSO [Fig. 5, Lanes 8 (312 nm) and 16 (365 nm), and Fig. 6, Lane 7 (visible light)]. The same trend was observed for compound **20** at 365 nm (Supporting Information, Figure S4.2).

Various nitro-aromatic derivatives were measured to have relatively large triplet yields and rapid radiationless decay via energy transfer (90,91). The formation of singlet molecular oxygen was found to occur upon irradiation of 7-nitro-1,4-benzodiazepines (92), whereas environmental toxicity of nitro-polyaromatic hydrocarbons has been attributed to reactive oxygen species and oxidative stress caused under sunlight (93).

A completely different behavior was observed for bromo derivative **18**. Its activity remained almost the same under argon and in the presence of radical scavengers. Some implication of singlet oxygen was also found (Fig. 6, Right image). Thus, it seems that the activity was most probably due to both homolysis of the C−Br bond as well as singlet oxygen formation pathway (37,38). Due to the similar nature and photocleavage at 312 nm between the bromo and the iodo quinazolinone derivatives (**18** and **19**, respectively, Fig. 2) we assume the same mode of action for compound **19**.

Photochemical experiments

Compounds which photocleave DNA should be able to form a DNA-compound type of "complex" via various intermolecular forces (53). The affinity to DNA obviously changes their photochemistry as compared to that in solution at the absence of the macromolecule. Nevertheless, some mechanistic aspects may, indeed, be clarified. The following photochemical experiments aimed to observe a possible reactivity of the NO_2 groups or homolysis of the C−Br bond. Any information was validated in order to further verify the observed photobiological results (Figs. 5 and 6).

In this context, compounds **15** and **18** were irradiated at 312 nm for 30, 60 and 120 min under air and under Argon (after careful degassing of the solutions) in a deuterated solvent (DMSO−d_6). ^{1}H−NMR spectroscopy was used to check all samples and the changes were compared to nonirradiated samples. As far as compound **15** concerns, we could observe no changes in our samples by ^{1}H−NMR, neither in the presence nor in its absence (see Supporting Information, Figure S5.1). For compound **18**, under both conditions, we could observe in the spectrum the appearance of some new low-intensity peaks which correspond probably to compound **12**, meaning that there was a tendency of quinazolinone **18** to lose bromine radical. However, this transformation occurs very slowly, under these conditions (see Supporting Information, Figure S5.2). Therefore, it seems that irradiation in DMSO solutions most probably does not cause any change to the compounds. This finding is in accordance with the blank experiments shown in Fig. 2 and verifies that DMSO does not affect, individually, either the plasmid DNA at the concentrations used or the compounds at any concentration, upon irradiation. However, the experiments shown below, in environments able to provide hydrogen species indicated a different behavior profile.

The tendency of 1,4−cyclohexadiene to supply hydrogen atoms (conversion to benzene) could be used to determine whether our compounds may abstract hydrogen atoms. If this is proved true, then the compounds should have the possibility to

react similarly, with DNA. Compounds **15**, **18** and **20** were left to react with 1,4−cyclohexadiene in dry benzene under argon, upon irradiation at 312 nm for 2 h. As expected, we observed no change in the ^{1}H−NMR spectra of the crude reaction mixture of compounds **15** and **20**, and LC−MS analysis showed peaks of the starting material and only traces of other compounds (Supporting Information, Figures S6 and S7). However, the ^{1}H−NMR spectrum of the reaction mixture of bromo derivative **18** had extra peaks, which correspond to the C−Br homolysis derivative **12** (Supporting Information, Figure S8).

The extent of conversion of compound **18** was better noticeable when experiments were performed changing the solvent to MeOH/H_2O (9/1) under irradiation at 312 nm for 2 h. By analyzing with LC−MS we observed the appearance of two bands of ions at 4.5−5.4 min which correspond to unreacted compound **18** and the newly formed derivative **12**. The same results were observed in the ^{1}H−NMR spectrum of the crude irradiated mixture. The ratio of compounds **12** and **18** was 1/1 (ratio of the corresponding hydrogen peaks, see Supporting Information, Figure S8). In general, homolysis of the C−halogen bond was found to be the driving force and the cause of DNA damage in other halogenated DNA photocleavers, (37,38) as well. No such homolysis was realized under irradiation at 365 nm, due to the lack of UV absorbance of the compound. Both nitro derivatives **15** and **20**, showed no change by ^{1}H−NMR and LC−MS analysis under either UVB or UVA irradiation when subjected to similar experimental conditions.

Biological assays

Cell culture experiments. Glioblastoma and melanoma are aggressive lethal human tumors for which the search for the improvement of therapeutic protocols as well as the understanding of their biochemical pathways is of our high interest. (94–99) Thus, the possible photocytotoxic effect of compound **15** against glioblastoma T98G and U87MG as well as melanoma A−375 cell lines has been evaluated.

The Resazurin Cell Viability Assay (CA035, Canvax, Spain) was used for cytotoxicity studies. This is a reliable, simple, non-toxic and safe method for cell viability based on the metabolic activity of cells to reduce resazurin to resorufin. In brief, cells seeded on well plates were incubated with 50 μμ of **15** and then irradiated at 365 nm using a UVA lamp for 1 and 2 h. Control cells were also irradiated with UVA for 2 h.

In glioblastoma cell lines it was observed that **15** did not affect cells' viability in dark (Fig. 7, 2nd and 5th column from left to right). Its cytotoxic effect appeared after irradiation and it is time dependent since it is increased, significantly after 2 h of UVA irradiation. Nevertheless, cytotoxicity was higher for T98G rather than U87MG. UVA irradiation did not affect cells' viability (data not shown).

Similarly, **15** was not cytotoxic for A375 cells without UVA irradiation (Fig. 8). However, A375 cell population was reduced dramatically when followed incubation with **15** and UVA irradiation. Control A375 cell lines population has been reduced by 60% when simply irradiated with UVA, while only 1−5% of cells survived when incubation with **15** was combined with UVA irradiation. Cytotoxic effect of **15** was weaker when cells were irradiated after removal of **15**. This is an indication that, during the experimental incubation time, compound **15** may enter cells and cause some damage, upon irradiation. Nevertheless, it seems that the remaining of the compound in the cell growth medium is able to cause further damage, probably on cell's membranes or other organelles,

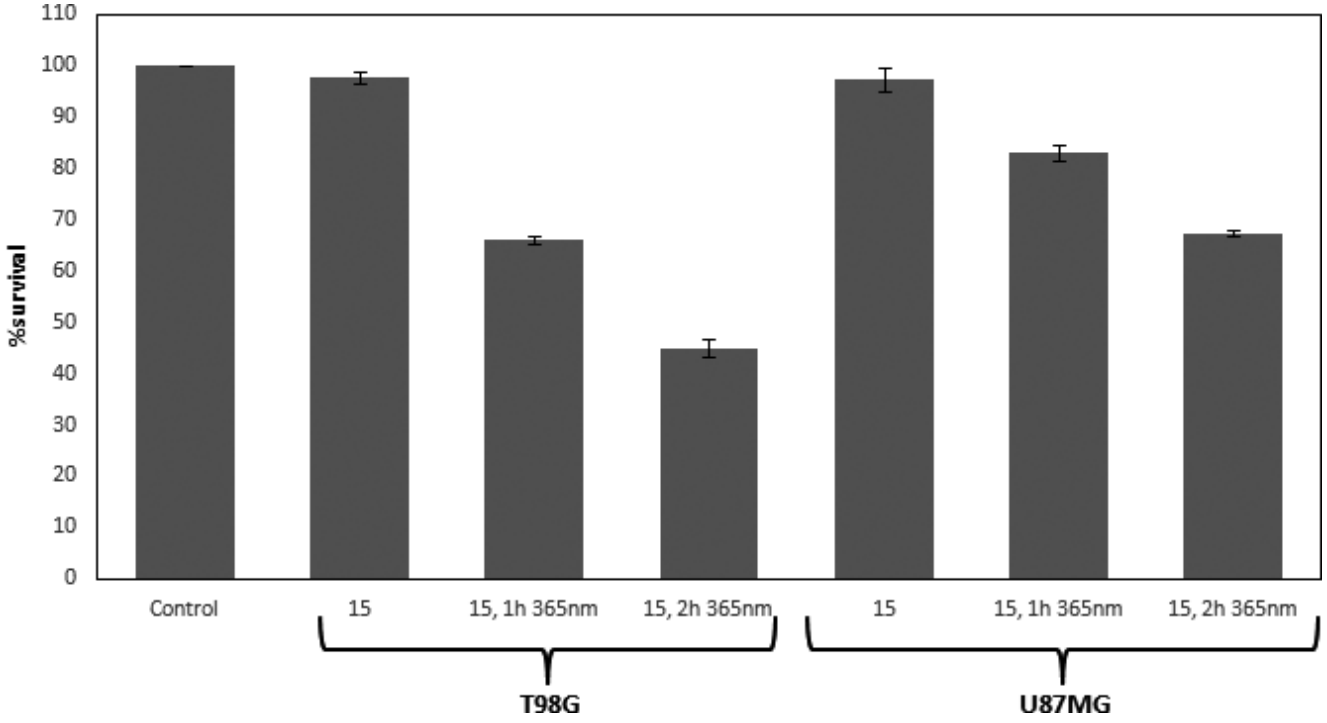

Figure 7. Cytotoxic effect of compound **15** against T98G and U87MG cell lines.

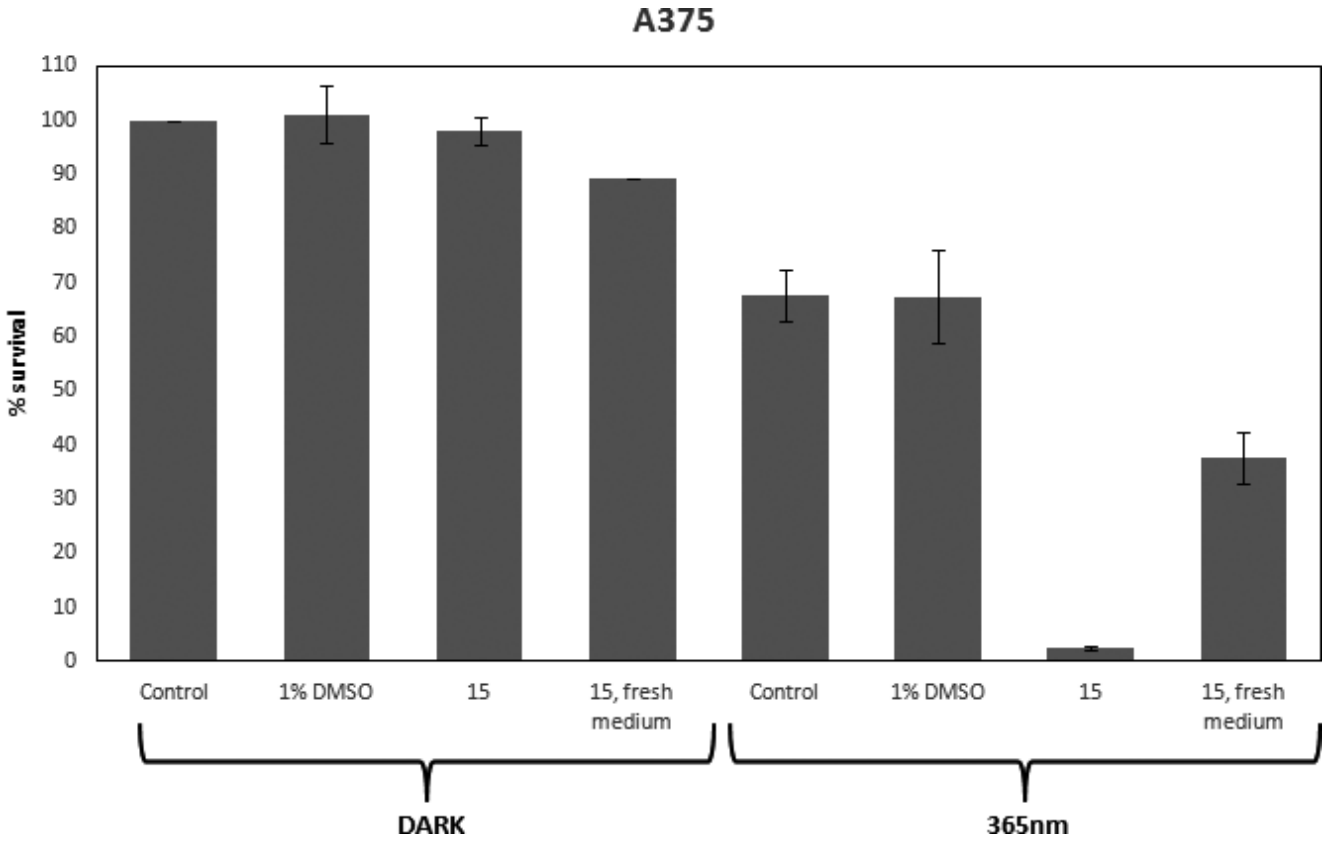

Figure 8. Cytotoxic effect of compound **15** against A375 melanoma cell line.

making, thus, compound **15** a promising tool for further photodamaging studies.

CONCLUSION

Eleven quinazolinones were synthesized in a one-step procedure from cheap readily available anthranilic acids, in very good yields and purity, using a green microwave irradiation mediated approach. Screening of these compounds in the presence of pBR322 plasmid DNA under UVB, UVA and visible light revealed four very effective DNA photocleavers, being time and concentration dependent and pH independent. Oxygen was participating on the DNA photocleavage; however, it was crucial for the nitro derivatives, indicating a possible photodynamic behavior.

Parent quinazolinone **12**, as well as 6−Me (**13**) and 6−OH derivatives (**14**) were not active. On the contrary, 6−bromo derivative **18** (and most probably iodo derivative **19**) exhibited its reactivity upon UVB irradiation via C−halogen bond homolysis as well as via singlet oxygen. Fluoro and chloro derivatives showed limited activity. Comparing the 6−or 7−chloro quinazolinones it becomes evident that substitution at position 6 is important for photoreactivity. The same was concluded for 6−and 7−nitro derivatives **15** and **20**, respectively. Addition of a second halogen atom, as in the case of 6,8−di−bromo derivative **22** resulted in a considerable reduction of the photosensitivity.

6−Nitro derivative **15** was highly active at UVB, UVA (at concentrations even below 10 μM) and visible light, whereas 7−nitro derivative **20** showed considerable activity at UVA and visible light. Formation of reactive oxygen species was found to be responsible for their activity. Nitro derivative **15**, which exhibited the best profile, was further tested in cells. It was found to be a very efficient *in vitro* photosensitizer for skin malignant melanoma cell line A−375, whereas its activity against two glioblastoma cell lines (U87MG and T98) was moderate.

Conclusively, it seems, that certain substituted quinazolinones, bearing a Br, I or NO_2 atom/group at position 6, may serve as new lead photosensitizers for the development of promising biotechnological applications and as novel photochemo and photodynamic therapeutics. Additionally, the designing of novel pharmaceutics based on certain quinazolinones should take into consideration their possible photoreactivities.

Acknowledgements—Part of this work was realized using the facilities of Hellenic Small Molecules Center (Aristotle University of Thessaloniki), partner of OPENSCREEN−GR (MIS 5002691), which is implemented under the Action "Reinforcement of the Research and Innovation Infrastructure," funded by the Operational Program "Competitiveness, Entrepreneurship and Innovation" (NSRF 2014-2020) and co-financed by Greece and the European Union (European Regional Development Fund).

SUPPORTING INFORMATION

Additional supporting information may be found online in the Supporting Information section at the end of the article:

Data S1. Data for quinazolinones **12**−**22**.

Data S2. Copies of NMR spectra of quinazolinones **12**−**22**.

Data S3. UV−Vis spectra of quinazolinones **12**−**22**.

Data S4. Gel electrophoresis studies: Figure S4.1. Compound **15**, study under various pH, Figure S4.2. Compound **20**, mechanistic study at 365 nm.

Data S5. ^{1}H NMR spectra of compounds **15** and **18** after irradiation in DMSO−d_6 at 312 nm: Figure S5.1. Compound **15**, Figure S5.2. Compound **18**.

Data S6. ^{1}H NMR spectra and LC-MS analysis of compound **15** after irradiation a) in MeOH/H_2O at 365 nm, b) in MeOH/H_2O at 312 nm, and c) in benzene with 1,4-cyclohexadiene.

Data S7. ^{1}H NMR spectra and LC-MS analysis of compound **20** after irradiation a) in MeOH/H_2O at 365 nm, b) in MeOH/H_2O at 312 nm, and c) in benzene with 1,4-cyclohexadiene.

Data S8. ^{1}H NMR spectra and LC-MS analysis of compound **18** after irradiation a) in MeOH/H_2O at 365 nm, b) in MeOH/H_2O at 312 nm, and c) in benzene with 1,4-cyclohexadiene.

Data S9. Fluorescence spectra of quinazolinones **12**−**22**.

REFERENCES

1. Garritsen, F. M., M. W. D. Brouwer, J. Limpens and P. I. Spuls (2014) Photo(chemo)therapy in the management of atopic dermatitis: An updated systematic review with implications for practice and research. *Br. J. Dermatol.* **170**, 501–513.
2. Marrani, E., I. Foeldvari, J. A. Lopez, R. Cimaz and G. Simonini (2018) Comparing ultraviolet light A photo(chemo)therapy with Methotrexate protocol in childhood localized scleroderma: Evidence from systematic review and meta-analysis approach. *Semin. Arthritis Rheum.* **48**, 495–503.
3. Dobson, J., G. F. de Queiroz and J. P. Golding (2018) Photodynamic therapy and diagnosis: Principles and comparative aspects. *Vet. J.* **233**, 8–18.
4. Spring, B. Q., I. Rizvi, N. Xu and T. Hasan (2015) The role of photodynamic therapy in overcoming cancer drug resistance. *Photochem. Photobiol. Sci.* **14**, 1476–1491.
5. Xiao, Q., J. Wu, X. Pang, Y. Jiang, P. Wang, A. W. Leung, L. Gao, S. Jiang and C. Xu (2018) Discovery and development of natural products and their derivatives as photosensitizers for photodynamic therapy. *Curr. Med. Chem.* **25**, 839–860.
6. Kataoka, H., H. Nishie, N. Hayashi, M. Tanaka, A. Nomoto, S. Yano and T. Joh (2017) New photodynamic therapy with next-generation photosensitizers. *Ann. Transl. Med.* **5**, art No 183.
7. Fan, W., P. Huang and X. Chen (2016) Overcoming the Achilles' heel of photodynamic therapy. *Chem. Soc. Rev.* **45**, 6488–6519.
8. Zhang, J., C. Jiang, J. P. Figueiró Longo, R. B. Azevedo, H. Zhang and L. A. Muehlmann (2018) An updated overview on the development of new photosensitizers for anticancer photodynamic therapy. *Acta Pharm. Sin. B.* **8**, 137–146.
9. Cho, S. J., S. Y. Kim, S. J. Park, N. Song, H. Y. Kwon, N. Y. Kang, S. H. Moon, Y. T. Chang and H. J. Cha (2016) Photodynamic approach for teratoma-free pluripotent stem cell therapy using CDy1 and visible light. *ACS Cent. Sci.* **2**, 604–607.
10. Saravanakumar, G., J. Lee, J. Kim and W. J. Kim (2015) Visible light-induced singlet oxygen-mediated intracellular disassembly of polymeric micelles co-loaded with a photosensitizer and an anticancer drug for enhanced photodynamic therapy. *Chem. Commun.* **51**, 9995–9998.
11. Lv, R., C. Zhong, R. Li, P. Yang, F. He, S. Gai, Z. Hou, G. Yang and J. Lin (2015) Multifunctional anticancer platform for multimodal imaging and visible light driven photodynamic/photothermal therapy. *Chem. Mater.* **27**, 1751–1763.
12. Gupta, J., J. Mohapatra and D. Bahadur (2017) Visible light driven mesoporous Ag-embedded ZnO nanocomposites: reactive oxygen species enhanced photocatalysis, bacterial inhibition and photodynamic therapy. *Dalton Trans.* **46**, 685–696.
13. Yang, M. F. and E. D. Baron (2008) Update on the immunology of UV and visible radiation therapy: Phototherapy, photochemotherapy and photodynamic therapy. *Expert Rev. Dermatol.* **3**, 85–98.
14. Grimes, D. R. (2017) Dose quantification in UV phototherapy. *Adv. Exp. Med. Biol.* **996**, 349–360.
15. Herzinger, T., M. Berneburg, K. Ghoreschi, H. Gollnick, E. Hölzle, H. Hönigsmann, P. Lehmann, T. Peters, M. Röcken, K. Scharffetter-Kochanek, T. Schwarz, J. Simon, A. Tanew and M. Weichenthal (2016) S1-Guidelines on UV phototherapy and photochemotherapy. *J. Dtsch Dermatol. Ges.* **14**, 853–876.
16. Reichrath, J., R. Saternus and T. Vogt (2017) Challenge and perspective: the relevance of ultraviolet (UV) radiation and the Vitamin D endocrine system (VDES) for psoriasis and other inflammatory skin diseases. *Photochem. Photobiol. Sci.* **16**, 433–444.
17. de Gruijl, F. R. (2016) For better or for worse, UV in psoriasis. *Exp. Dermatol.* **25**, 945–946.
18. Bagherani, N. (2016) The efficacy of 308 nm UV excimer light as monotherapy and combination therapy with topical khellin 4% and/or tacrolimus 0.1% in the treatment of vitiligo. *Dermatol. Ther.* **29**, 137–138.
19. Kim, S. R., H. Heaton, L. Y. Liu and B. A. King (2018) Rapid repigmentation of vitiligo using tofacitinib plus low-dose, narrowband UV-B phototherapy. *JAMA Dermatol.* **154**, 370–371.
20. Su, L. N., J. Ren, S. M. Cheng, J. L. Liu, Y. F. Ding and N. W. Zhu (2017) UVA1 vs. narrowband UVB phototherapy in the treatment of palmoplantar pustulosis: a pilot randomized controlled study. *Lasers Med. Sci.* **32**, 1819–1823.
21. Kuo, Y. H. and C. H. Chang (2016) Erythrodermic mycosis fungoides treated with low-dose methotrexate and 311 nm UV-B: A case report with 3-year follow up and literature review. *Dermatol. Sin.* **34**, 37–41.
22. Wang, J., C. J. Perry, K. Meeth, D. Thakral, W. Damsky, G. Micevic, S. Kaech, K. Blenman and M. Bosenberg (2017) UV-induced somatic mutations elicit a functional T cell response in the YUMMER1.7 mouse melanoma model. *Pigment Cell Melanoma Res.* **30**, 428–435.
23. Balevi, A., P. Üstüner, S. A. Kakşi and M. Özdemir (2018) Narrowband UV-B phototherapy: An effective and reliable treatment alternative for extensive and recurrent pityriasis versicolor. *J. Dermatolog. Treat.* **29**, 252–255.
24. Wiegell, S. R., U. B. Johansen and H. C. Wulf (2019) Pulse–daylight–photodynamic therapy in combination with corticosteroid and brimonidine tartrate for multiple actinic keratoses: A randomized clinical trial. *Acta Derm. Venereol.* **99**, 242–243.
25. Grandi, V., I. Baldi, P. Cappugi, M. Mori and N. Pimpinelli (2016) Indole 3-acetic acid-photodynamic therapy in the treatment of multiple actinic keratoses: A proof of concept pilot study. *Photodiagnosis Photodyn. Ther.* **16**, 17–22.
26. Safar, R., A. Alkhars, M. Tallegas, N. Korsaga-Some and L. Machet (2019) Successful treatment for extensive bowen's disease using daylight-mediated photodynamic therapy. *Acta Derm. Venereol.* **99**, 701–702.
27. Morton, C. A., R. M. Szeimies, A. Sidoroff and L. R. Braathen (2013) European guidelines for topical photodynamic therapy part 1: Treatment delivery and current indications - Actinic keratoses, Bowen's disease, basal cell carcinoma. *J. Eur. Acad. Dermatol. Venereol.* **27**, 536–544.
28. Ma, L. W., K. P. Nielsen, V. Iani and J. Moan (2007) A new method for photodynamic therapy of melanotic melanoma - Effects of depigmentation with violet light photodynamic therapy. *J. Environ. Pathol. Toxicol. Oncol.* **26**, 165–172.
29. Serini, S. M., M. V. Cannizzaro, A. Dattola, V. Garofalo, E. Del Duca, A. Ventura, M. Milani, E. Campione and L. Bianchi (2019) The efficacy and tolerability of 5-aminolevulinic acid 5% thermosetting gel photodynamic therapy (PDT) in the treatment of mild-to-moderate acne vulgaris. A two-center, prospective assessor-blinded, proof-of-concept study. *J. Cosmet. Dermatol.* **18**, 156–162.
30. Hamblin, M. R. (2016) Antimicrobial photodynamic inactivation: a bright new technique to kill resistant microbes. *Curr. Opin. Microbiol.* **33**, 67–73.
31. Maisch, T. (2015) Resistance in antimicrobial photodynamic inactivation of bacteria. *Photochem. Photobiol. Sci.* **14**, 1518–1526.
32. Al-Ahmad, A., C. Tennert, L. Karygianni, K. T. Wrbas, E. Hellwig and M. J. Altenburger (2013) Antimicrobial photodynamic therapy

using visible light plus water-filtered infrared-A (wIRA). *J. Med. Microbiol.* **62**, 467–473.
33. Aggarwal, R., G. Sumran, V. Kumar and A. Mittal (2011) Copper (II) chloride mediated synthesis and DNA photocleavage activity of 1-aryl/heteroaryl-4-substituted-1,2,4-triazolo[4,3-a]quinoxalines. *Eur. J. Med. Chem.* **46**, 6083–6088.
34. Sumran, G., R. Aggarwal, A. Mittal, A. Aggarwal and A. Gupta (2019) Design, synthesis and photoinduced DNA cleavage studies of [1,2,4]-triazolo[4,3-a]quinoxalin-4(5H)-ones. *Bioorg. Chem.* **88**, art No 102932.
35. Yang, W. Y., S. Roy, B. Phrathep, Z. Rengert, R. Kenworthy, D. A. R. Zorio and I. V. Alabugin (2011) Engineering pH-gated transitions for selective and efficient double-strand DNA photocleavage in hypoxic tumors. *J. Med. Chem.* **54**, 8501–8516.
36. Mandal, S. and A. Basak (2009) Aza Hopf cyclization: synthesis and reactivity of cyclic azadieneynes. *Tetrahedron Lett.* **50**, 3641–3644.
37. Jeon, R. and P. A. Wender (2001) Photocleavage of DNA by 4′-Bromoacetophenone Analogs. *Arch. Pharm. Res.* **24**, 39–43.
38. Liu, D., G. Yuan and J. Hu (2006) Synthesis and photo-induced DNA cleaving activities of conjugates of halophenyl derivative and polyamide containing N-methylimidazoles. *J. Photochem. Photobiol. B, Biol.* **82**, 187–193.
39. Qian, X., Y. Li, Y. Xu, Y. Liu and B. Qu (2004) Highly-efficient DNA photocleavers with long wavelength absorptions: Thio-heterocyclic fused naphthalimides containing aminoalkyl side chains. *Bioorg. Med. Chem. Lett.* **14**, 2665–2668.
40. Zhou, J., C. Fang, Y. Liu, Y. Zhao, N. Zhang, X. Liu, F. Wang and D. Shangguan (2015) Visible-light-induced cleavage of 4-α-amino acid substituted naphthalimides and its application in DNA photocleavage. *Org. Biomol. Chem.* **13**, 3931–3935.
41. Saito, I., M. Takayama and S. Kawanishi (1995) Photoactivatable DNA-cleaving amino acids: highly sequence-selective DNA photocleavage by novel L-lysine derivatives. *J. Am. Chem. Soc.* **117**, 5590–5591.
42. Nielsen, P. E., C. Jeppesen, M. Egholm and O. Buchardt (1988) Photochemical cleavage of DNA by nitrobenzamides linked to 9-aminoacridine. *Biochemistry* **27**, 6338–6343.
43. Nielsen, P. E., M. Egholm, T. Koch, J. B. Christensen and O. Buchardt (1991) Photolytic cleavage of DNA by nitrobenzamido ligands linked to 9-aminoacridines gives DNA polymerase substrates in a wavelength-dependent reaction. *Bioconjug. Chem.* **2**, 57–66.
44. Naik, T. R., H. S. Naik, H. R. Naik, P. J. Bindu, B. G. Harisha and V. Krishna (2009) Synthesis, DNA binding, docking and photocleavage studies of novel benzo[b][1,8]naphthyridines. *Med. Chem.* **5**, 411–418.
45. Bindu, P. J., K. M. Mahadevan and T. R. Ravikumar Naik (2012) An efficient one-pot synthesis and photoinduced DNA cleavage studies of 2-chloro-3-(5-aryl-4,5-dihydroisoxazol-3-yl)quinolines. *Bioorg. Med. Chem. Lett.* **22**, 6095–6098.
46. Bindu, P. J., K. M. Mahadevan and T. R. Ravikumar Naik (2012) Sm(III)nitrate-catalyzed one-pot synthesis of furano[3,2c]-1,2,3,4-tetrahydroquinolines and DNA photocleavage studies. *J. Mol. Struct.* **1020**, 142–147.
47. Bindu, P. J., K. M. Mahadevan, T. R. Ravikumar Naik and B. G. Harish (2014) Synthesis, DNA binding, docking and photocleavage studies of quinolinyl chalcones. *MedChemComm* **5**, 1708–1717.
48. Chowdhury, N., S. Dutta, B. Nishitha, S. Dasgupta and N. D. P. Singh (2010) N, O-Diacyl-4-benzoyl-N-phenylhydroxylamines as photoinduced DNA cleaving agents. *Bioorg. Med. Chem. Lett.* **20**, 5414–5417.
49. Chowdhury, N., S. Dutta, S. Dasgupta, N. D. Singh, M. Baidya and S. K. Ghosh (2012) Synthesis, photophysical, photochemical, DNA cleavage/binding and cytotoxic properties of pyrene oxime ester conjugates. *Photochem. Photobiol. Sci.* **11**, 1239–1250.
50. Hwu, J. R., S. C. Tsay, S. C. Hong, M. H. Hsu, C. F. Liu and S. S. P. Chou (2013) Relationship between structure of conjugated oxime esters and their ability to cleave DNA. *Bioconjug. Chem.* **24**, 1778–1783.
51. Bindu, P. J., K. M. Mahadevan, N. D. Satyanarayan and T. R. Ravikumar Naik (2012) Synthesis and DNA cleavage studies of novel quinoline oxime esters. *Bioorg. Med. Chem. Lett.* **22**, 898–900.
52. Karamtzioti, P., A. Papastergiou, J. G. Stefanakis, A. E. Koumbis, I. Anastasiou, M. Koffa and K. C. Fylaktakidou (2015) O-Benzoyl pyridine aldoxime and amidoxime derivatives: Novel efficient DNA photo-cleavage agents. *MedChemComm* **6**, 719–726.
53. Pasolli, M., K. Dafnopoulos, N. P. Andreou, P. S. Gritzapis, M. Koffa, A. E. Koumbis, G. Psomas and K. C. Fylaktakidou. (2016) Pyridine and p-nitrophenyl oxime esters with possible photochemotherapeutic activity: Synthesis, DNA photocleavage and DNA binding studies. *Molecules*, **21**, art No 864.
54. Papastergiou, A., S. Perontsis, P. Gritzapis, A. E. Koumbis, M. Koffa, G. Psomas and K. C. Fylaktakidou (2016) Evaluation of O-alkyl and aryl sulfonyl aromatic and heteroaromatic amidoximes as novel potent DNA photo-cleavers. *Photochem. Photobiol. Sci.* **15**, 351–360.
55. Andreou, N. P., K. Dafnopoulos, C. Tortopidis, A. E. Koumbis, M. Koffa, G. Psomas and K. C. Fylaktakidou (2016) Alkyl and aryl sulfonyl p-pyridine ethanone oximes are efficient DNA photo-cleavage agents. *J. Photochem. Photobiol. B, Biol.* **158**, 30–38.
56. Gritzapis, P. S., N.-P. Andreou, K. R. Katsani, K. Dafnopoulos, G. Psomas, Z. V. Peitsinis, A. E. Koumbis and K. C. Fylaktakidou (2020) p-Pyridinyl oxime carbamates: Synthesis, DNA binding, DNA photocleaving activity and theoretical photodegradation studies. *Beilstein J. Org. Chem.* **16**, 337–350.
57. Guan, H., X. Liu, W. Peng, R. Cao, Y. Ma, H. Chen and A. Xu (2006) β-carboline derivatives: Novel photosensitizers that intercalate into DNA to cause direct DNA damage in photodynamic therapy. *Biochem. Biophys. Res. Commun.* **342**, 894–901.
58. Kovvuri, J., B. Nagaraju, V. L. Nayak, R. Akunuri, M. P. N. Rao, A. Ajitha, N. Nagesh and A. Kamal (2018) Design, synthesis and biological evaluation of new β-carboline-bisindole compounds as DNA binding, photocleavage agents and topoisomerase I inhibitors. *Eur. J. Med. Chem.* **143**, 1563–1577.
59. Kumar, V., K. Kaur, D. N. Karelia, V. Beniwal, G. K. Gupta, A. K. Sharma and A. K. Gupta (2014) Synthesis and biological evaluation of some 2-(3,5-dimethyl-1H-pyrazol-1- yl)-1-arylethanones: Antibacterial, DNA photocleavage, and anticancer activities. *Eur. J. Med. Chem.* **81**, 267–276.
60. Nishiwaki, E., H. Lee, T. Matsumoto, K. Toyooka, H. Sakurai and M. Shibuya (1990) Synthesis of nitrated oligo-N-methylpyrrole carboxamide derivatives and their photochemical DNA cleaving activities. *Tetrahedron Lett.* **31**, 1299–1302.
61. Chowdhury, N., S. Dutta, S. Karthick, A. Anoop, S. Dasgupta and N. D. Pradeep Singh (2012) Azido carbonyl compounds as DNA cleaving agents. *J. Photochem. Photobiol. B, Biol.* **115**, 25–34.
62. Jafari, E., M. R. Khajouei, F. Hassanzadeh, G. H. Hakimelahi and G. A. Khodarahmi (2016) Quinazolinone and quinazoline derivatives: Recent structures with potent antimicrobial and cytotoxic activities. *Res. Pharm. Sci.* **11**, 1–14.
63. Khan, I., A. Ibrar, W. Ahmed and A. Saeed (2015) Synthetic approaches, functionalization and therapeutic potential of quinazoline and quinazolinone skeletons: The advances continue. *Eur. J. Med. Chem.* **90**, 124–169.
64. Khan, I., A. Ibrar, N. Abbas and A. Saeed (2014) Recent advances in the structural library of functionalized quinazoline and quinazolinone scaffolds: Synthetic approaches and multifarious applications. *Eur. J. Med. Chem.* **76**, 193–244.
65. Khan, I., S. Zaib, S. Batool, N. Abbas, Z. Ashraf, J. Iqbal and A. Saeed (2016) Quinazolines and quinazolinones as ubiquitous structural fragments in medicinal chemistry: An update on the development of synthetic methods and pharmacological diversification. *Bioorg. Med. Chem.* **24**, 2361–2381.
66. Connolly, D. J., D. Cusack, T. P. O'Sullivan and P. J. Guiry (2005) Synthesis of quinazolinones and quinazolines. *Tetrahedron* **61**, 10153–10202.
67. Parua, S., S. Das, R. Sikari, S. Sinha and N. D. Paul (2017) One-pot cascade synthesis of quinazolin-4(3H)-ones via nickel-catalyzed dehydrogenative coupling of o-aminobenzamides with alcohols. *J. Org. Chem.* **82**, 7165–7175.
68. Peng, X. M., L. P. Peng, S. Li, S. R. Avula, V. K. Kannekanti, S. L. Zhang, K. Y. Tam and C. H. Zhou (2016) Quinazolinone azolyl ethanols: Potential lead antimicrobial agents with dual action modes targeting methicillin-resistant Staphylococcus aureus DNA. *Future Med. Chem.* **8**, 1927–1940.
69. Peng, L. P., S. Nagarajan, S. Rasheed and C. H. Zhou (2015) Synthesis and biological evaluation of a new class of quinazolinone azoles as potential antimicrobial agents and their interactions with

calf thymus DNA and human serum albumin. *MedChemComm* **6**, 222–229.
70. Malecki, N., P. Carato, B. Rigo, J. F. Goossens, R. Houssin, C. Bailly and J. P. Hénichart (2004) Synthesis of condensed quinolines and quinazolines as DNA ligands. *Bioorg. Med. Chem.* **12**, 641–647.
71. Ovchinnikova, I. G., G. A. Kim, E. G. Matochkina, M. I. Kodess, P. A. Slepukhin, I. S. Kovalev, E. V. Nosova, G. L. Rusinov and V. N. Charushin (2018) Synthesis, photochemical and luminescent properties of ortho-hydroxystyrylquinazolinone-linked benzocrown ethers. *J. Photochem. Photobiol. A, Chem.* **351**, 16–28.
72. Ovchinnikova, I. G., G. A. Kim, E. G. Matochkina, M. I. Kodess, N. V. Barykin, O. S. Eĭtsov, E. V. Nosova, G. L. Rusinov and V. N. Charushin (2014) Synthesis, photochemical and luminescent properties of (E)-2-(2-hydroxyarylethylene)-3-phenylquinazolin-4(3H)-ones. *Russ. Chem. Bull.* **63**, 2467–2477.
73. Hricovíni, M. and M. Hricovíni (2017) Photochemically-induced anti-syn isomerization of quinazolinone-derived Schiff's bases: EPR, NMR and DFT analysis. *Tetrahedron* **73**, 252–261.
74. Maiti, S., J. Kim, J. H. Park, D. Nam, J. B. Lee, Y. J. Kim, J. M. Kee, J. K. Seo, K. Myung, J. U. Rohde, W. Choe, O. H. Kwon and S. Y. Hong (2019) Chemoselective trifluoroethylation reactions of quinazolinones and identification of photostability. *J. Org. Chem.* **84**, 6737–6751.
75. Tokura, Y., M. Ogai, H. Yagi and M. Takigawa (1994) Afloqualone photosensitivity. Immunogenicity of Afloqualone-photomodified epidermal cells. *Photochem. Photobiol.* **60**, 262–267.
76. Fujita, H. and I. Matsuo (1987) Phototoxic potential of afloqualone, a quinazolinone derivative, as determined by photosensitized inactivation of bacteriophage. *Chem. Biol. Interact.* **64**, 139–149.
77. Fujita, H. and I. Matsuo (1988) UV-A induced DNA nicking activities of skin photosensitive drugs: Phenothiazines, benzothiadiazines and afloqualone. *Chem. Biol. Interact.* **66**, 27–36.
78. Tanizawa, H., Y. Taking, T. Oku, H. Hashizumi, Y. Iwamoto and T. Itoyama (1992) Photodynamic deoxyribonucleic acid (DNA) strand breaking activities of enoxacin and afloqualone. *Chem. Pharm. Bull.* **40**, 1868–1870.
79. Lazou, M., A. Tarushi, P. Gritzapis and G. Psomas (2020) Transition metal complexes with a novel guanine-based (E)-2-(2-(pyridin-2-ylmethylene)hydrazinyl)quinazolin-4(3H)-one: Synthesis, characterization, interaction with DNA and albumins and antioxidant activity. *J. Inorg. Biochem.* **206**, art No 111019.
80. Kakoulidou, C., P. S. Gritzapis, A. G. Hatzidimitriou, K. C. Fylaktakidou and G. Psomas (2020) Zn(II) complexes of (E)-4-(2-(pyridin-2-ylmethylene)hydrazinyl)quinazoline in combination with non-steroidal anti-inflammatory drug sodium diclofenac: Structure, DNA binding and photo-cleavage studies, antioxidant activity and interaction with albumin. *J. Inorg. Biochem.* **211**, art No 111194.
81. Mitrakas, A. G., D. Kalamida and M. I. Koukourakis (2014) Effect of mitochondrial metabolism-interfering agents on cancer cell mitochondrial function and radio/chemosensitivity. *Anticancer Drugs* **25**, 1182–1191.
82. Zachari, M. A., P. S. Chondrou, S. E. Pouliliou, A. G. Mitrakas, I. Abatzoglou, C. E. Zois and M. I. Koukourakis (2014) Evaluation of the alamarblue assay for adherent cell irradiation experiments. *Dose-Response* **12**, 246–258.
83. Rad-Moghadam, K. and M. Mohseni (2003) An expeditious and solvent-free route to the synthesis of 2-substituted quinazolin-4(3H)-ones under microwave conditions. *J. Chem. Res.* S 487–488.
84. Kulkarni, S. S., S. Singh, J. R. Shah, W. K. Low and T. T. Talele (2012) Synthesis and SAR optimization of quinazolin-4(3H)-ones as poly(ADP-ribose)polymerase-1 inhibitors. *Eur. J. Med. Chem.* **50**, 264–273.
85. Alexandre, F. R., A. Berecibar and T. Besson (2002) Microwave-assisted Niementowski reaction. Back to the roots. *Tetrahedron Lett.* **43**, 3911–3913.
86. Armitage, B. (1998) Photocleavage of nucleic acids. *Chem. Rev.* **98**, 1171–1200.
87. Cadet, J., S. Mouret, J. L. Ravanat and T. Douki (2012) Photoinduced damage to cellular DNA: Direct and photosensitized reactions. *Photochem. Photobiol.* **88**, 1048–1065.
88. Ma, A. and X. Dai (2018) The relationship between DNA single-stranded damage response and double-stranded damage response. *Cell Cycle* **17**, 73–79.
89. Strauss, B. S. (2018) Why is dna double stranded? The discovery of dna excision repair mechanisms. *Genetics* **209**, 357–366.
90. Hurley, R. and A. C. Testa (1968) Triplet-state yield of aromatic nitro compounds. *J. Am. Chem. Soc.* **90**, 1949–1952.
91. Döpp, D. (1975) Reactions of aromatic nitro compounds via excited triplet states. In *Triplet States II*. (Edited by Wild U.P., Döpp D., Dürr H. Topics Curr. Chem. **55**, 49–85.Springer, Berlin, Heidelberg.
92. Cornelissen, P. J. G. and G. M. J. B. Van Henegouwen (1981) Photochemical activity of 7-nitro-1,4-benzodiazepines - Formation of singlet molecular oxygen, isolation and identification of decomposition products. *Pharm. Weekbl. Sci. Ed.* **3**, 800–809.
93. Onduka, T., D. Ojima, K. Ito, K. Mochida, M. Ito, J. Koyama and K. Fujii (2017) Photo-induced toxicity and oxidative stress responses in Tigriopus japonicus exposed to nitro-polycyclic aromatic hydrocarbons and artificial light. *Chemosphere* **169**, 596–603.
94. Mitrakas, A. G., D. Kalamida, A. Giatromanolaki, S. Pouliliou, A. Tsolou, R. Kyranas and M. I. Koukourakis (2018) Autophagic flux response and glioblastoma sensitivity to radiation. *Cancer Biol. Med.* **15**, 260–274.
95. Koukourakis, M., A. Tsolou, S. Pouliliou, I. Lamprou, M. Papadopoulou, M. Ilemosoglou, G. Kostoglou, D. Ananiadou, E. Sivridis and A. Giatromanolaki (2017) Blocking LDHA glycolytic pathway sensitizes glioblastoma cells to radiation and temozolomide. *Biochem. Biophys. Res. Commun.* **491**, 932–938.
96. Koukourakis, M. I., A. G. Mitrakas and A. Giatromanolaki (2016) Therapeutic interactions of autophagy with radiation and temozolomide in glioblastoma: Evidence and issues to resolve. *Br. J. Cancer* **114**, 485–496.
97. Giatromanolaki, A., E. Sivridis, N. E. Bechrakis, G. Willerding, G. S. Charitoudis, M. H. Foerster, K. C. Gatter, A. L. Harris and M. I. Koukourakis (2012) Phosphorylated pVEGFR2/KDR receptor expression in uveal melanomas: Relation with HIF2α and survival. *Clin. Exp. Metastasis* **29**, 11–17.
98. Giatromanolaki, A. N., G. S. Charitoudis, N. E. Bechrakis, V. P. Kozobolis, M. I. Koukourakis, M. H. Foerster and E. L. Sivridis (2011) Autophagy patterns and prognosis in uveal melanomas. *Mod. Pathol.* **24**, 1036–1045.
99. Sivridis, E., M. I. Koukourakis, S. E. Mendrinos, A. Karpouzis, A. Fiska, C. Kouskoukis and A. Giatromanolaki (2011) Beclin-1 and LC3A expression in cutaneous malignant melanomas: A biphasic survival pattern for beclin-1. *Melanoma Res.* **21**, 188–195.